Residual order within thermally grown amorphous SiO_2 on crystalline silicon

K. Tatsumura,[1,*] T. Watanabe,[1,2] D. Yamasaki,[1] T. Shimura,[3] M. Umeno,[4] and I. Ohdomari[1,5]
[1]*School of Science and Engineering, Waseda University, 3-4-1 Ohkubo, Shinjuku-ku, Tokyo 169-8555, Japan*
[2]*PRESTO, Japan Science and Technology Agency, 4-1-8 Honcho, Kawaguchi-shi, Saitama 332-0012, Japan*
[3]*Department of Material and Life Science, Graduate School of Engineering, Osaka University, 2-1 Yamadaoka, Suita-shi, Osaka 565-0871, Japan*
[4]*Department of Management Science,Faculty of Engineering, Fukui University of Technology, 3-6-1 Gakuen, Fukui-shi, Fukui 910-8505, Japan*
[5]*Kagami Memorial Laboratory for Materials Science and Technology, Waseda University, 2-8-26 Nishi-waseda, Shinjuku-ku, Tokyo 169-0051, Japan*

(Received 10 November 2003; revised manuscript received 8 December 2003; published 27 February 2004)

The origin of x-ray diffraction peaks observed on the crystal truncation rods (CTR's) in reciprocal space for thermally grown SiO_2 films has been investigated by large-scale atomistic simulation of silicon oxidation. Three models of SiO_2 on Si(001), Si(111), and Si(113) were formed by introducing oxygen atoms in crystalline Si from the surfaces in an atom-by-atom manner. The SiO_2 structures are classified as being amorphous in conventional characterizations, but retain the residual order originating from the {111} atomic planes in their parent crystals. The calculated diffraction patterns exhibit intensity peaks with Laue-function-like fringe profiles along the CTR's, at positions depending on the substrate orientations, agreeing quite well with experimental results.

DOI: 10.1103/PhysRevB.69.085212 PACS number(s): 68.55.Jk, 61.10.Eq, 61.43.Bn, 81.65.Mq

I. INTRODUCTION

The thermally grown SiO_2 on crystalline Si (c-Si) is an almost perfect insulator, primarily responsible for the predominance of silicon in the microelectronics industry. The structure of the thermal oxide is amorphous as far as one can see by using electron diffraction[1] and infrared absorption spectrum.[1] A fundamental problem that remains with the SiO_2/Si interface is the mechanism of structural order decay with transition from the crystalline Si to the amorphous SiO_2 (a-SiO_2). Several studies of high-resolution transmission electron microscopy (HRTEM) and grazing incidence x-ray scattering have indicated the presence of a boundary layer of microcrystallites[2,3] and an epitaxial interfacial layer.[4,5] However, several TEM studies have supported an abrupt crystalline-amorphous change at the interface.[6,7] These earlier studies have focused primarily on order at or near the SiO_2/Si interface, while recent x-ray diffraction studies have provided direct evidence of structural order throughout the bulk SiO_2.[8–12] This evidence consists of weak diffraction peaks observed on the crystal truncation rods (CTR's) in reciprocal space, where the CTR is caused by the termination of crystalline Si lattice at the interface. The width of the peak in the direction perpendicular to the CTR is almost the same as that of the CTR scattering from the substrate.[11] The profile of the peak along the CTR exhibits an oscillation fringe pattern of which the period corresponds to the inverse of the oxide thickness.[11] These characteristic features of the peak mean that the whole structure of the oxide film has some structural order having an epitaxial relationship with the substrate.

For thermal oxides on Si(001), Si(110), and Si(111), such diffraction peaks have been observed on the CTR's extending from the 111 Bragg points.[11] Since the direction of the CTR is normal to the truncated surface of the crystal lattice, the positions of the peaks in reciprocal space are quite different depending on the substrate orientations. For deposited SiO_2 films, no diffraction peak has been observed on the CTR's.[12] These results indicate that the structure of the thermal oxide is influenced by the Si lattice from which it was formed.

The purpose of this paper is to theoretically clarify the origin of the diffraction peaks on the CTR's for thermal oxide films. The number of nonequivalent diffraction peaks observed on the CTR's so far is only one for SiO_2/Si(001) and Si(110) and two for SiO_2/Si(111),[11] therefore it is impossible to do an ordinary structural analysis from the diffraction data. The alternative we take here is first to build realistic models of thermal oxide on c-Si and then to examine diffraction properties of the models together with other structural properties.

II. CALCULATION METHOD

In order to deal with a model large enough to describe the amorphous nature of the oxide, we use the interatomic potential function designed for Si, O, mixed systems, previously developed by us.[13,31] The potential function is an extended version of the Stillinger-Weber potential for pure Si systems.[14]

The initial simulation structures are silicon single crystals. The (001)-terminated Si model (4800 atoms) is 6.51-nm thick along [001] and 3.84-nm long along $[1\bar{1}0]$ and [110]. The (111)-terminated Si model (4840 atoms) is 6.27-nm thick along [111] and 4.22-nm long along $[\bar{1}10]$ and $[\bar{1}01]$. The (113)-terminated Si model (4680 atoms) is 6.38-nm thick along [113], 3.84-nm long along $[1\bar{1}0]$ and 3.82-nm long along $[33\bar{2}]$. The two-dimensional periodic boundary condition is adopted in directions parallel to the surface. The simulation-cell size and atoms at the bottom layer are fixed, but this constraint does not prohibit the volumetric expansion

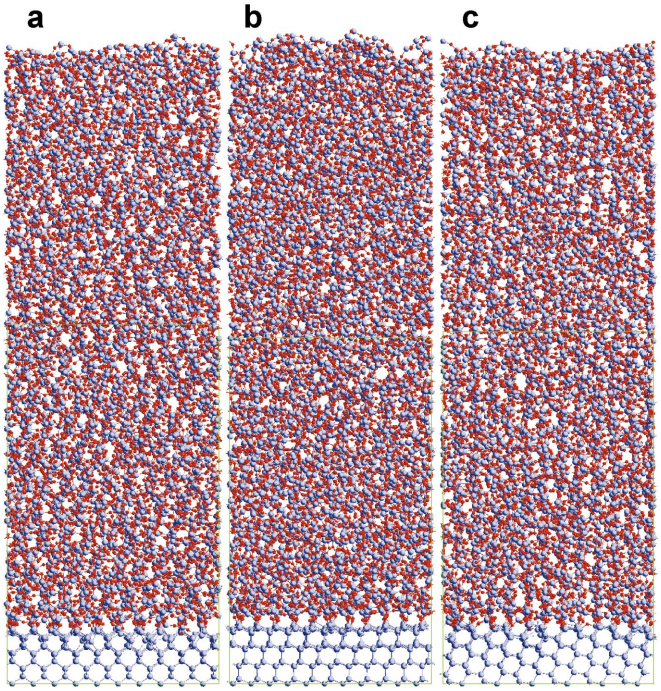

FIG. 1. (Color) Large-scale models of thermal oxide films on c-Si. (a) SiO_2/Si(001) (12 536 atoms), (b) SiO_2/Si(111) (12 248), and (c) SiO_2/Si(113) (12 124). Blue and red spheres represent Si and O atoms, respectively.

toward the surface-normal direction.

Starting from the c-Si models, the SiO_2 models are formed by inserting the O atoms, atom-by-atom, directly into the Si-Si bonds. The dynamical aspect of oxidation process, such as adsorption, dissociation, and diffusion of the oxidant, are also important, but they are beyond the scope of this paper. The insertion procedure of O atoms is prescribed based on the experimental evidences that show the layer-by-layer oxidation of c-Si (Refs. 7 and 15) and the compositionally abrupt interface.[16,17] Oxidation starts from the top monolayer and oxidation of the next monolayer is suppressed until the upper monolayers are fully oxidized. The Si-Si bond to be oxidized next is chosen at random from all those above the interface at each stage. After every insertion step of oxygen atoms, the structure is optimized to remove the artificial high strain energy due to the short Si-O bond length at the insertion site. At every interval of 20 insertions ($\sim$0.1 ML), molecular dynamics (MD) calculation is performed for 20 000 steps ($\sim$0.76 ps) maintaining the temperature at 1073 K by Nose method.[18] A time step of 2.30 $\times 10^{-5}$ ps is used with fifth order of Gear's algorithm[19] to solve numerically Nose's equation of motion. The potential function used allows each atom to break a bond or to form a new bond with another atom according to the exerted force. In the simulation, the high pressure occurring during the oxidation process may be relieved by structural rearrangements causing bond breaking, leading to a disordered silica network.

III. RESULTS AND DISCUSSION

Figure 1 shows the finally obtained SiO_2/Si models in

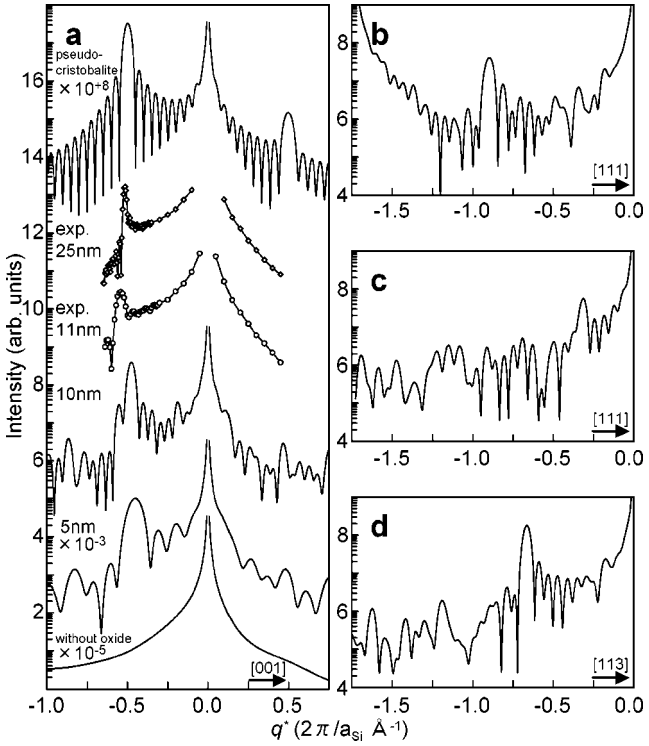

FIG. 2. X-ray diffraction intensities calculated for the SiO_2/Si models (Fig. 1). Data are plotted on a log scale as a function of q^*, where q^* is the distance along the CTR from the 111 Bragg point in silicon reciprocal lattice unit. (a) Scans of the 10-nm and 5-nm SiO_2 models on Si(001) along [001] where $q^*=0$ corresponds to 1,1,1, coupled with the data for the bare silicon substrate and the 10 nm pseudocristobalite/Si(001) model. Experimental spectra for 11-nm, 25-nm thick oxides (from Ref. 8) are also shown. (b) and (c) Scans of the 10-nm SiO_2 model on Si(111) along [111] ($q^*=0$ to 1,1,1 for b and to 1,1,-1 for c) (d) Scan of the 10-nm SiO_2 model on Si(113) along [113] ($q^*=0$ to 1,1,1).

$\langle 110 \rangle$ projection (oxide thickness = 10.4 nm). For the modeling on Si(001), Si(111), and Si(113), the total numbers of inserted O atoms are 7736, 7408, and 7444, and the total MD times amounts to 295.5, 282.2, and 284.8 ps, respectively.

Figure 2 shows the x-ray diffraction intensities calculated for the SiO_2/Si models by kinematical diffraction theory. The intensities are scanned along the CTR scattering extending from the 111 Bragg peaks. For the SiO_2 models of 10-nm and 5-nm thickness on Si(001) [Fig. 2(a)], there clearly exists an intensity peak at $q^*=-0.48$, corresponding to 1,1,0.52 in reciprocal space. Similar peaks appear at all four of the 1,1,0.52 equivalent positions, but other higher-order reflections are not seen.[20] The peak profile along the CTR consists of main and several subpeaks and exhibits a Laue-function-like oscillation-fringe pattern, namely, the width of the main peak is twice as much as that of subpeaks and the period (λ) of the oscillation in reciprocal space is related to the inverse of the corresponding film thickness (t) by $\lambda = a_{Si}/t$, where a_{Si} is the silicon unit-cell dimension. The Laue-function-shape peak profile is a typical diffraction pattern for crystalline thin films.[21] The peak profile together with the increase in the peak intensity with thickness means that the coherent scatterers are not limited to the interface,

but are present throughout the oxide film. Furthermore, it is confirmed by scans perpendicular to the CTR (Fig. 3) that the peak is exactly located on the CTR and that its width in the direction perpendicular to the CTR is the same as that of the CTR scattering, indicating that the coherent scatterers are well oriented to the substrate with an epitaxial relationship. Randomly oriented grains of scatterers would result in a spherical shell of scattering with a radius ($\sqrt{h^2+k^2+l^2}$) equal to the length of the 1,1,0.52 reciprocal vector (Debye-Scheller ring). Consequently, we can say that the positions and characteristics of the peaks are in good agreement with the experimental results.[8–12]

The pseudocristobalite/c-Si structure model,[11,22] depicted in Fig. 4(a), can serve as a basis for understanding the structure of the simulated SiO_2/Si models. The pseudocristobalite is obtained from a diamond lattice of Si atoms with oxygen between nearest Si neighbors by elongating its lattice spacing almost twice in the surface-normal direction. Therefore, the pseudocristobalite has the same network topology as the cristobalite and is fitted to the underlying Si lattice at the interface with an epitaxial relationship. In fact, the atom arrangement of the SiO_2 model averaged over the whole corresponds to the pseudocristobalite lattice; each atom is significantly displaced from the lattice position, but the total displacement vectors sum up to an almost zero vector.

Provided that a crystal lattice is enlarged by c in a direction, the corresponding reciprocal lattice shrinks by $1/c$ in the same direction. Therefore, the pseudocristobalite structure has the reciprocal lattice point ($\mathbf{G}'$) corresponding to each ($\mathbf{G}$) of that of c-Si: $\mathbf{G}'=1/c\ \mathbf{G}_{\parallel}+\mathbf{G}_{\perp}$, where c is the expansion ratio, $\mathbf{G}_{\parallel}$ the parallel component of $\mathbf{G}$ to the surface-normal direction, and $\mathbf{G}_{\perp}$ the perpendicular one. Note that $\mathbf{G}'$ is necessarily on the CTR from the Bragg point denoted by $\mathbf{G}$ [Fig. 4(c)].

The pseudocristobalite structure with $c=2$ shows a diffraction peak with the Laue-function-shape profile at 1,1,0.5 [Fig. 2(a) top]. This is a Bragg reflection from the (1,1,1/c) parallel planes in the pseudocristobalite, which are derived from the (111) atomic planes in the original c-Si [Fig. 4(b)]. The diffraction peak appearing at 1,1,0.52 for the SiO_2 model is essentially the same as the Bragg reflection at 1,1,0.5 for the pseudocristobalite, indicating that the SiO_2 model retains the *residual order* emanating from the (111) atomic planes in the original c-Si. The expansion ratio of the simulated SiO_2 model on Si(001) is estimated to be 1.92 by least-squares fitting to the pseudocristobalite. The residual order has a periodicity of 3.60 Å with the normal direction oriented to [1,1,0.52]. While there are large amounts of local static disorder, the residual order as a whole has the epitaxial relationship with the c-Si substrate. This is the reason that the peak shows characteristics similar to a Bragg reflection from the epitaxial crystalline thin film.

The significant displacement of each atom from the average lattice position explains the disappearance of higher-order Bragg reflections for the pseudocristobalite structure. As an example, the Bragg reflection of 1,1,1.5 derived originally from the (113) planes in c-Si can be seen at $q^*=0.5$ for the pseudocristobalite in the top of Fig. 2(a), but collapses for the SiO_2 model (also see supplementary data in Ref. 20). The root mean squares of the displacement, $\sqrt{\langle\delta^2\rangle}$, are estimated to be 1.59, 2.61, and 1.76 Å for the SiO_2 models on Si(001), Si(111), and Si(113), in this order. It can be qualitatively said that a set of parallel planes denoted by $\mathbf{G}$ will lose its periodicity with the interval ($d_{\mathbf{G}}$) of $2\pi/|\mathbf{G}|$, if each atom constructing the plane is displaced more than half the interval on average, so that the Bragg reflection from them will vanish. The displacement, more quantitatively, does not influence the peak position and its width, but does weaken its intensity by static Debye-Waller factor, $\exp\{(-2\pi^2/3)\langle\delta^2\rangle/d_{\mathbf{G}}^2\}$. The ratio of the displacement to the plane interval is exponentially effective and the estimated displacements are large compared with most plane intervals of Si lattice. The 111 reciprocal lattice point has the lowest index among all points that are not forbidden reflections, so that the {111} parallel planes have the longest intervals,

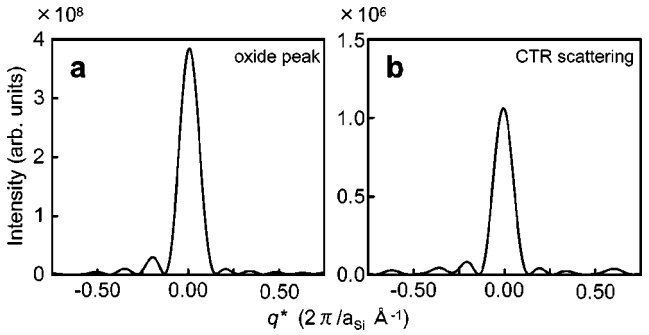

FIG. 3. Intensity profiles perpendicular to the CTR. Data are plotted on a liner scale as a function of q^*, where q^* is the distance from the CTR in [$1\bar{1}0$] ($q^*=0$ corresponds to 1,1,0.52). (a) For the 10-nm SiO_2/Si(001) model. (b) For the Si(001) substrate in the model of (a), that is, without the SiO_2 contribution. The oscillation fringe pattern is due to the finite model size in directions parallel to the surface.

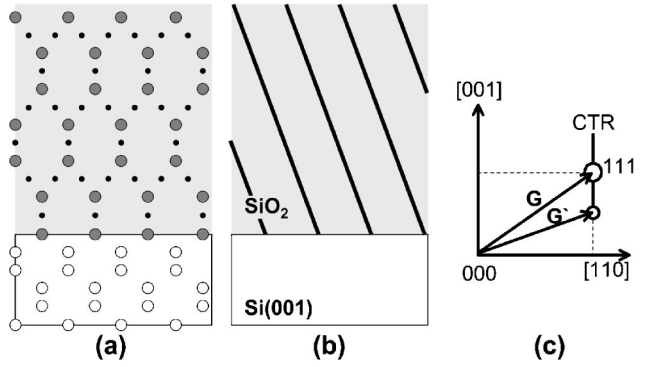

FIG. 4. (a) Side view of the pseudocristobalite/Si(001) model. Large and small spheres indicate Si and O atoms, respectively. (b) (1,1,1/c) parallel planes in the pseudocristobalite on Si(001), which are derived from the (111) atomic planes in the original c-Si by assuming the expansion in the surface-normal direction. Here, c is the expansion ratio of the pseudocristobalite to the original c-Si. (c) Schematic representation of reciprocal space around the 111 Bragg point.

3.14 Å, while the second one is 220, corresponding to plane intervals of 1.92 Å. It can be said that when Si lattice are oxidized with expansion in the surface-normal direction, the Bragg reflections derived originally from {111} planes in c-Si are most persistent against the displacement and can survive even if all the others disappear.

The same understanding stands for the cases of Si(111) and Si(113) substrates, but the corresponding pseudocristobalite structures[11] are fundamentally different from that of Si(001) because of the directions to elongate Si lattice. For the SiO_2 model on Si(111),[32] a diffraction peak appears on the CTR from the 111 point at 0.48,0.48,0.48 ($q^*=-0.90$) [Fig. 2(b)] and another diffraction peak appears on the CTR from the 111 point at 0.82,0.82,-1.18 ($q^*=-0.31$) [Fig. 2(c)], agreeing with experimental results.[11] These diffraction peaks appearing on the two independent CTR's indicate the residual order derived from the (111) and $(11\bar{1})$ planes in the original c-Si(111) with expansion in [111] of $c=2.05$. Here, the (111) plane is parallel to the Si(111) surface, while the $(11\bar{1})$ plane is at an angle of 70.5° to the surface.

For the SiO_2 model on Si(113), a diffraction peak appears on each of the three independent CTR's from the 111, $\bar{1}11$, and $1\bar{1}1$ points. These peaks are located at 0.80,0.80,0.40 ($q^*=-0.66$ from $\bar{1}11$) [Fig. 2(d)], -1.09, -1.09,0.73 ($q^*=-0.30$ from $\bar{1}11$) and 0.86,-1.14,0.57 ($q^*=-0.48$ from $1\bar{1}1$), indicating the residual order emanating from the (111), $(\bar{1}\bar{1}1)$, and $(1\bar{1}1)$ planes in the original c-Si(113). They are derived from the (111), $(\bar{1}11)$, and $(1\bar{1}\bar{1})$ planes by not only elongating the Si lattice in [113] with $c=1.98$ but also slightly shifting them in $[\bar{3}32]$ with a ratio of 0.9 Å per a length of 10 Å in [113]. This tilted direction is due to bond directions in plane of Si(113) that have lower symmetry than those of Si(001) and Si(111). After this prediction about the diffraction properties for the SiO_2/Si(113), we have confirmed the positions of these peaks experimentally.

The SiO_2 models should be called amorphous in conventional characterizations and are far from the pseudocristobalite crystal itself. The pair-correlation function [Fig. 5(a)], a reduced expression of the radial distribution function, shows five peaks in the short-distance side at positions coinciding with those of a-SiO_2,[23,24] indicating the short-range order of corner-sharing SiO_4 tetrahedrons. But in the long-distance side, it becomes almost 1 indicating the disappearance of two-body correlation. The pseudocristobalite is not stable in strain energy[25] and consists of unusually distorted bond angles of O-Si-O such as about 65° and 135°. The SiO_2 model has a distribution of O-Si-O bond angles centered at an almost tetrahedral angle, 109° and a distribution of Si-O-Si bond angles with an average value slightly narrower than the equilibrium bond angle in a-SiO_2, 144° [Fig. 5(b)]. Regarding the bonding network [Fig. 5(c)], it has similar ring statistics to that of a-SiO_2 and is different from the pseudocristobalite which contains only six-membered rings, where closed paths having n Si-O segments are referred to as n-membered rings. Furthermore, the disappearance of higher-order reflections,[20] in accordance with experimental

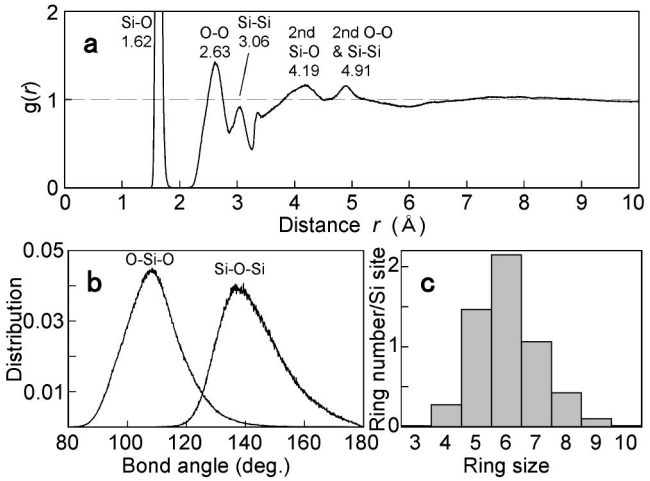

FIG. 5. Analyses of the SiO_2/Si(001) model at 300 K. (a) Pair-correlation function. (b) Bond angle distributions. (c) Ring statistics according to the shortest path analysis.[26]

results, is solid evidence of the SiO_2 models being sufficiently disordered to be comparable with the real materials, indicating that there is not any other order existing in the pseudocristobalite expect for one that we report in this work.

Since all the positions of the x-ray diffraction peaks depending on the substrate orientations and their characteristic features are reproduced by the present SiO_2/Si models, we conclude that thermal oxide films retain the residual order emanating from the {111} atomic planes in their parent crystals. Recent studies of HRTEM (Ref. 27) and angle-scanned photoelectron diffraction[28,29] have indicated the presence of pseudocristobalite-like structures at the interface. The x-ray diffraction properties described above reveals that the (partly) ordered oxide is not limited to the interface, but extends throughout the film with increasing local static disorder. The residual order tends to be decreased in the model grown at a higher temperature, 2000 K, and is removed after high-temperature annealing.[30] This is observed also in the x-ray diffraction.[30] The heat treatment at a higher temperature induces greater displacement of atoms from the average lattice positions and the resultant structure of the bond reconstruction approaches that of fused silica.

IV. SUMMARY

We performed large-scale atomistic modeling of thermally grown SiO_2 and obtained the SiO_2/Si models that reproduce x-ray diffraction peaks on the CTR's extending from the 111 Bragg points in reciprocal space, in accordance with experimental results. The SiO_2 models also show structural properties similar to the a-SiO_2 structure in terms of pair-correlation function, bond angle distributions and ring statistics, and are stable in strain energy. It was demonstrated that the SiO_2 models retain the residual order emanating from the {111} atomic planes in their parent crystals, without other order corresponding to higher-order index planes because of large amounts of local static disorder. The residual order as a whole bears an epitaxial relationship to the underlying Si substrate and yields the sharp diffraction peaks on CTR's.

ACKNOWLEDGMENTS

This work has been supported by a Grant-in-Aid for COE Research from the MEXT, Japan, partly by a Grant from JST-PRESTO, and by a grant for the promotion of the advancement of education and research in graduate schools from the Promotion and Mutual Aid Corporation for Private Schools of Japan. One of the authors (K.T.) has been funded by the Research Programs of the JSPS for Young Scientists. The synchrotron radiation experiments were performed at the Photon Factory.

*Electronic address: tatsumura@toki.waseda.jp

[1] N. Nagasima, Jpn. J. Appl. Phys. **9**, 879 (1970).
[2] P.H. Fuoss, L.J. Norton, S. Brennan, and A. Fischer-Colbrie, Phys. Rev. Lett. **60**, 600 (1988).
[3] F. Rochet, M. Froment, C. D'Anterroches, H. Roulet, and G. Dufour, Philos. Mag. B **59**, 339 (1989).
[4] A. Ourmazd, D.W. Taylor, J.A. Rentschler, and J. Bevk, Phys. Rev. Lett. **59**, 213 (1987).
[5] T.A. Rabedeau, I.M. Tidswell, P.S. Pershan, J. Bevk, and B.S. Freer, Appl. Phys. Lett. **59**, 706 (1991).
[6] H. Akatsu, Y. Sumi, and I. Ohdomari, Phys. Rev. B **44**, 1616 (1991).
[7] F.M. Ross and J.M. Gibson, Phys. Rev. Lett. **68**, 1782 (1992).
[8] I. Takahashi, T. Shimura, and J. Harada, J. Phys.: Condens. Matter **5**, 6525 (1993).
[9] A. Munkholm, S. Brennan, F. Comin, and L. Ortega, Phys. Rev. Lett. **75**, 4254 (1995); T. Shimura, M. Umeno, I. Takahashi, and J. Harada, *ibid.* **79**, 4932 (1997); A. Munkholm, S. Brennan, F. Comin, and L. Ortega, *ibid.* **79**, 4933 (1997).
[10] N. Awaji, Y. Sugita, Y. Hori, and I. Takahashi, Appl. Phys. Lett. **74**, 2669 (1999).
[11] T. Shimura, T. Hosoi, and M. Umeno, in *The Physics and Chemistry of* SiO_2 *and the* Si-SiO_2 *Interface-4,* edited by H.Z. Massoud, I.J.R. Baumvol, M. Hirose, and E.H. Poindexter (Electrochemical Soc., Pennington, 2000), Vol. 2000-2, p. 241; T. Shimura *et al., ibid.,* Vol. 96-1, p. 456.
[12] T. Shimura, H. Sensui, and M. Umeno, Cryst. Res. Technol. **33**, 637 (1998).
[13] T. Watanabe, H. Fujiwara, H. Noguchi, T. Hoshino, and I. Ohdomari, Jpn. J. Appl. Phys. Part 2 **38**, L366 (1999).
[14] F.H. Stillinger and T.A. Weber, Phys. Rev. B **31**, 5262 (1985).
[15] H. Watanabe, K. Kato, T. Uda, K. Fujita, M. Ichikawa, T. Kawamura, and K. Terakura, Phys. Rev. Lett. **80**, 345 (1998).
[16] M.T. Sieger, D.A. Luh, T. Miller, and T.-C. Chiang, Phys. Rev. Lett. **77**, 2758 (1996).
[17] D.-A. Luh, T. Miller, and T.-C. Chiang, Phys. Rev. Lett. **79**, 3014 (1997).
[18] S. Nose, Mol. Phys. **52**, 255 (1984).
[19] C.W. Gear, *Numerical Initial Value Problems in Ordinary Differential Equations* (Prentice-Hall, New Jersey, 1971).
[20] See EPAPS Document No. E-PRBMDO-69-037408 for the x-ray diffraction intensity distributions along the CTR's (00*l*, 11*l*, 20*l*, 22*l*, etc.). A direct link to this document may be found in the online article's HTML reference section. The document may also be reached via the EPAPS homepage (http://www.aip.org/pubservs/epaps.html) or from ftp.aip.org in the directory/epaps/. See the EPAPS homepage for more information.
[21] See, for examples, D.K. Bowen and B.K. Tanner, *High Resolution X-ray Diffractometry and Topography* (Taylor and Francis, London, 1998).
[22] T. Hattori, T. Igarashi, M. Ohi, and H. Yamagishi, Jpn. J. Appl. Phys. Part 2 **28**, L1436 (1989).
[23] P.A.V. Johnson, A.C. Wright, and R.N. Sinclair, J. Non-Cryst. Solids **58**, 109 (1983).
[24] B.P. Feuston and S.H. Garofalini, J. Chem. Phys. **89**, 5818 (1988).
[25] T. Yamasaki, C. Kaneta, T. Uchiyama, T. Uda, and K. Terakura, Phys. Rev. B **63**, 115314 (2001).
[26] J.P. Rino, I. Ebbsjö, R.K. Kalia, A. Nakano, and P. Vashishta, Phys. Rev. B **47**, 3053 (1993).
[27] N. Ikarashi, K. Watanabe, and Y. Miyamoto, Phys. Rev. B **62**, 15 989 (2000).
[28] S. Dreiner, M. Schürmann, C. Westphal, and H. Zacharias, Phys. Rev. Lett. **86**, 4068 (2001).
[29] C. Westphal, Appl. Phys. A **76**, 721 (2003).
[30] K. Tatsumura, T. Watanabe, D. Yamasaki, T. Shimura, M. Umeno, and I. Ohdomari, Jpn. J. Appl. Phys. Part 1 **42**, 7250 (2003).
[31] T. Watanabe and I. Ohdomari, Thin Solid Films **343-344**, 370 (1999).
[32] K. Tatsumura, T. Watanabe, D. Yamasaki, T. Shimura, M. Umeno, and I. Ohdomari, Jpn. J. Appl. Phys. Part 1 **43**, 492 (2004).